Estimation of Volume of An Eastern Himalayan Glacier Using A Novel Method Based On The Ice Surface Velocity Data And Basal Sliding Velocity

Dr. Anubha Agrawal

Abstract - A novel method is developed to find the volume of a valley glacier. The main methods for volume estimation are volume-area scaling, GlabTop, ITEM and surface velocity method. None of these methods calculates the basal sliding velocity. The new method developed estimates basal sliding velocity at every point where thickness calculation is performed. The fraction f of the gravitational driving stress causing the shear deformation of glacier ice is assumed to depend on the surface slope and basal slip ratio. The value of factor f is calculated using the correction factors reported in a study based on the finite element simulations of Stokes equations. This method of volume estimation does not require digitization of central flowlines and can be used to automatically calculate volume of a glacier from the surface slope and ice velocity data.

Keywords - Volume, Basal Sliding Velocity, Longitudinal Stress Gradients, Glacier.

I. INTRODUCTION

Ice volume estimates are important for assessing the glacier health and also the water reserves stored in glaciers. Measuring the ice-thickness distribution of a glacier and finding an estimate of its total volume by means of borehole measurements and radio-echo soundings is expensive and difficult because of topographical constraints. Due to this, off-field methods are increasingly being used for the volume estimation of glaciers. Farinotti et al. (2009) named their method as Ice-Thickness Estimation Method (ITEM). They calculated ice-flux using mass balance and elevation change data; ice-flux was subsequently used to estimate the ice thickness at the central flowline. McNabb et al. (2012) used surface velocity data in addition to the data used by Farinotti et al. (2009), while Morlighem et al. (2011) and Brinkerhoff et al. (2016) used sparse ice-thickness data as well for finding the ice-thickness distribution. Cooper et al. (2010), Linsbauer et al. (2012) etc. estimated ice thickness using surface slope data and the assumptions of perfect plastic flow and constant basal shear stress. Linsbauer et al. (2012) termed their method as Glacier Bed Topography (GlabTop). All these methods are based on the calculation of ice thickness along a set of ice flowlines that determine the main ice-flow path through the glacier. Gantayat et al. (2014) estimated ice thickness at points over the entire glacier surface using the ice surface velocity data and the modified SIA velocity equation; but they assumed a uniform basal velocity for the entire glacier in their calculations of ice thickness. Frey et al. (2014) suggested a variation of GlabTop method where thicknesses were calculated on the randomly picked Digital Elevation Model (DEM) cells on the glacier surface, and the volume of glacier was estimated by an averaging process, thus avoiding the digitization of central flowlines.

All the above methods are based on the shear-deformational models based on SIA. The SIA approach neglects lateral drag and longitudinal stress in the calculation of ice flowline velocity. Nye (1965) had introduced a shape factor f in his calculation of ice flowline velocity to account for the effect of lateral drag due to the side walls of the glacier valley. In the same spirit, Adhikari and Marshall (2011) proposed a longitudinal stress factor L; the $L-$factor was the product of two components, namely (1) the deformational factor L_d, and (2) the sliding factor L_s. They estimated the longitudinal stress factor L_d based on the correction factor required to match the flowline surface velocity calculated from the modified SIA equation with that from the Finite element simulation of plane strain Stokes equations. They modelled the bedrock as a flat surface of uniform slope, and the ice profile along the flowline direction as a flattened half-circle. Because of the longitudinal stress gradients (LSG), the vertical shear stress required to balance the gravitational driving stress is modified. The factor L_d was based on the change in the shear deformation of ice due to the longitudinal stress gradients when the basal velocity was assumed as zero. They also calculated the slip-based longitudinal stress factor L_s. The factor L_s quantified the effect of slip on the contribution of longitudinal stress gradients in resisting the driving stress. They obtained an expression for L_d in terms of the bedrock slope, and also tabulated the values of L_s for different slip ratios and sliding length to maximum thickness ratios. In this paper, slip ratio, i.e. the ratio of sliding velocity and deformational velocity of ice, is estimated by an iterative process. These values of L_s and L_d are used in the present work to find the part of driving stress producing the deformational component of ice surface velocity.

In this paper, the effect of lateral drag is incorporated by assuming a constant value of Nye shape factor $f_n = 0.8$ for all glaciers. It is also assumed that lateral drag provides uniform resistance to the flow across the width. If the cross-section shape varies slowly along the flowline, the influence of lateral drag may be assumed to be constant along the length of the glacier as well. Haeberli and Hoelzle (1995) chose $f_n = 0.8$ for the entire glacier in their parametrization scheme. Linsbauer et al. (2012) and Frey et al. (2014) also chose a constant shape factor value of 0.8 for all glaciers when calculating volumes by the GlabTop method.

Locally, the basal drag along with longitudinal stress gradients and lateral drag balances the gravitational driving stress. So the overall shape factor f used in this work is taken as equal to the product of factors f_n, L_s and L_d; it thus provides the factor for finding the effective driving stress, which is used in the modified SIA velocity equation for thickness calculation. Adhikari and Marshall (2011, 2012) did not combine the effects of LSG and lateral drag in one single factor; their modified flowline model dealt with the effect of either lateral drag or LSG at a time.

Meur and Vincent (2003) applied a two-dimensional (2-D) ice-flow model based on SIA to investigate the dynamics of Glacier de Saint-Sorlin, France. They emphasised the need of incorporating LSG to capture the small-scale dynamics represented by ice surface velocities, while the large-scale dynamics represented by volume or length changes could be reproduced accurately by their SIA model because the longitudinal effects from short-scale disturbances cancel out over horizontal distances of several times the ice thickness. Vincent et al. (2000) concluded using 1-D SIA model that the sliding velocity cannot be described by Weertman analysis or empirical relations connecting sliding velocity to thickness and surface slope; they had calculated sliding velocity from the difference of observed surface velocity and calculated deformational velocity. Meur et al. (2004) found using a 3-D simulation of a glacier with an inclined sine-shaped symmetrical bedrock that LSG explained a large part of the misfit between the SIA and the full-Stokes finite element results. The finite element models solving the full-stress Stokes equations can account for the contributions from all deviatoric components to the flow pattern, but 3-D models may not be the best choice due to the large uncertainties in the input data of glacier geometry. Kamb and Echelmeyer (1986) showed that the bedrock bumps can locally change the flow pattern by transmitting LSG over the distances of the order of several times the ice thickness, thus affecting the validity of SIA. Van der Veen et al. (2014) found in their study on Byrd glacier, East Antarctica that small-scale variations in driving stress are only partially balanced by LSG, resulting in a wave-like pattern of basal drag indicating spatial variations in basal conditions. Truffer (2004) developed an inverse method to calculate the basal motion of a glacier, and he found that true basal velocities cannot be recovered because of the diffusive nature of ice flow; also, an attempt to fit the surface velocities exactly creates unrealistic oscillations in the basal velocity solution. Van der Veen and Whillans (1989a) pioneered the force-budget method and calculated the basal velocities by solving momentum equations in successive layers starting from the input data of surface velocity and moving to the bedrock; the calculated basal velocities were more sensitive to the small errors in the input data of surface velocity; also basal shear stresses showed unrealistic oscillations on the short scale though their variation was smoother on the larger scale of several ice thicknesses. All the above points to the difficulties involved in any attempt to find the short-scale variation of basal velocity and basal stresses, though LSG can be helpful in describing the short-scale variation of surface velocity.

Finding basal velocities is a classic ill-posed problem as different assumptions for the basal velocity field can lead to the same surface velocities; the boundary conditions are surplus at the glacier surface and insufficient at the ice-bed interface. Also theoretical sliding laws do not perform well on a macroscopic scale, which otherwise would have made the system of equations soluble. So there is a need to assess the basal velocity by a method that uses the local data of surface velocity and mean slope, and also accounts for the integrated effect of large-scale dynamics on surface velocity; this is what has been attempted in this paper. Also in this paper, the aim is to estimate the thickness distribution and volume of a glacier, rather than the basal velocity distribution.

This paper utilizes the slope and ice surface velocity data derived from satellite pictures. Ice thickness can be calculated for points on the flowline or every pixel of the glacier surface using the proposed method. This method of calculation of ice-thickness of a glacier is tested on Nisqually glacier, a valley glacier on the south side of Mount Rainier, Washington. The calculations are also performed for the glaciers, namely, Dokriani and Zemu. The average thickness values obtained are compared with the reported results. This method is then used to estimate the volume of the East Rathong glacier, Sikkim Himalaya.

The method's uncertainty is governed by the uncertainties in the values of creep factor A and limiting basal shear stress value τ_b. The value of τ_b used in this work is based on the empirical expression by Haeberli and Hoelzle (1995). The value of creep parameter A is based on the assumption of a temperate glacier and is taken as constant for a glacier. Mainly two values have been used in this work for A, i.e. 2.4×10^{-24} and 3.4×10^{-24} Pa^{-3} s^{-1}. The value 2.4×10^{-24} Pa^{-3} s^{-1} for creep parameter was used by Farinotti et al. (2009) for the volume estimation of Swiss glaciers. Also uncertainties in the input data of slope and ice surface velocity are the other sources of error. But the addition of pixel volumes should lead to the cancellation of random errors on average. The scatter of results based on the typical uncertainty ranges $(\tau_b : \pm 40\,\%, A : \pm 35\,\%)$ is within ±10% of the mean value. The value of creep parameter A can be treated as a tuning parameter if the Ground Penetrating RADAR (GPR) thickness data for the glacier is available. The method has the potential to calculate the volume of the large glacier systems with less manual effort as glacier boundaries and flowlines need not be digitized.

II. STUDY AREA

The current study is based on East Rathong glacier which is located in the Sikkim Himalaya. It is a summer nourished and south-east facing glacier. The glacier is divided into three distinct zones: accumulation zone (Ac) (slope = -0.45), ablation zone (Ab) (slope= -0.13), and a transition zone (slope = -0.55) connecting the accumulation and ablation zones of the glacier. The transition zone covers an elevation range of > 1000 m in the total altitudinal range of 2000 m for the East Rathong glacier. The mean elevation of the ablation zone of the glacier is 4700 m a.s.l. and the mean elevation of the accumulation zone of the glacier is 6200 m a.s.l. The length of the glacier is 6300 m.

III. DATA SETS

I. Cartosat-1

The Department of Space (DOS), Government of India, launched the Cartosat-1 satellite on 5th May'05. It is the first Indian Remote Sensing Satellite capable of providing in-orbit satellite images, and is designed for cartography applications. It has a polar sun-synchronous orbit and makes 1867 orbits with a 126 day cycle. It is used for the stereo viewing of large scale mapping and terrain modelling applications. The satellite provides high resolution near-instantaneous stereo data. It has a spatial resolution of 2.5 m and radiometric resolution of 10 bit quantization. The satellite carries two PAN sensors with fore-aft stereo capability. The high resolution stereo data can be used to generate a high-quality DEM. The DEM, C1_DEM_16b_2006-2008_V1_88E27N_G45E for Sikkim glaciers, used in this study, has been downloaded from http://bhuvan3.nrsc.gov.in/bhuvan/bhuvannew/bhuvan2d.php.

II. Landsat

Landsat 8 is an American Earth Observatory Satellite launched on 11 February 2013. The Landsat 8 Operational Land Imager (OLI) and Thermal Infrared Sensor (TIRS) images consist of nine spectral bands with a spatial resolution of 30 meters for Bands 1 to 7 and 9. The new band 1 is for coastal and aerosol studies and the new band 9 is for cirrus cloud detection. The resolution for the band 8 (panchromatic) is 15 meters. The thermal bands 10 and 11 are for providing surface temperatures, collected at 100 meters resolution.

The cloud-free and seasonal snow free Landsat8 images acquisitioned on 20th Nov'13, and 28th March'14 have been downloaded from the Earth explorer (http://earthexplorer.usgs.gov/).

The data sets used in the study are summarized in Table 1.

Table 1: Details of the satellite data analysed in the study

Date	Sensor	Mission	Path/ Row	Pixel Res (m)
20 Nov 2013	OLI	Landsat 8 (band 8)	139/41	15
28 March 2014	OLI	Landsat 8 (band 8)	139/41	15
2006-2008	PAN	Cartosat-1 DEM		2.5

IV. METHODOLOGY

The purpose of the method is to find the ice-thickness distribution given the ice surface velocity and slope data of the glacier. The proposed methodology is explained below in six sub-sections:

I. Modified Shallow Ice Approximation Equation

The shallow ice approximation (SIA) approach neglects lateral and longitudinal stresses. In this work the modified 1-D SIA model incorporates the effects of lateral and longitudinal stress gradients by the use of a shape factor f.

The glacier is taken as a parallel-sided slab of thickness H with the inclination angle (α) of surface and bed-rock as same. Ice is assumed to deform as an incompressible, non-linear viscous material under self-weight with the vertical shear stress τ_{xz} at centerline varying as $f\rho g(H-z)\sin\alpha$. Here z is the perpendicular distance of a point from the bedrock, and the *x*-coordinate is measured along the length of the glacier. The density of ice ρ is taken as 900 kg m^{-3}, and the acceleration due to gravity g is 9.81 m s^{-2}. The glacier ice is assumed to follow Glen's flow rule with the exponent $n=3$. Ice flows by the phenomenon of creep due to vertical shear stress, and thus acquires a velocity called the deformational velocity. The ice surface velocity u_s is the sum of deformational velocity u_d and basal velocity u_b. There exist analytical solutions for ice velocities in isothermal, laminar flow (e.g. Cuffey and Patterson 2010). The expression of surface velocity at any point on the flowline is:

$$u_s = \frac{2A}{n+1}\left(f\rho g\sin\alpha\right)^n H^{n+1} + u_b$$
$$= (1+\phi)\frac{2A}{n+1}\left(f\rho g\sin\alpha\right)^n H^{n+1} \qquad (1)$$

The creep parameter *A* is known to depend mainly on the ice temperature and water content. Its value may require tuning with the help of GPR thickness data, or it may be a depth-averaged value based on the temperature profile measured in a borehole and empirical relations relating temperature and creep parameter.

A term that is crucial in Eq. (1) is the slip ratio value which is unknown. Slip ratio ϕ is defined as the ratio between sliding velocity and deformational velocity. Other unknowns are: f and H. The variables surface slope α and surface velocity u_s are provided as the input data obtained from the satellite images.

II. Calculation of basal sliding velocity

The modified shallow ice Eq. (1) assumes the vertical shear stress as $f\rho g(H-z)\sin\alpha$. So the value of basal shear stress used in deriving the expression of surface velocity turns out to be $f\rho gH\sin\alpha$. But the limiting value of basal shear stress τ_b for a glacier is nearly constant as explained by Lliboutry's theory on sliding, bed erosion and cavitation, Fowler (2010). Also the longitudinal stress gradients keep basal drag fairly uniform by balancing the variations in driving stress required to maintain flux continuity over an irregular bed surface, Van der Veen et al. (2014).

The short scale bed-rock variations are filtered by the glacier when transmitting them to the surface. The effect of bedrock undulations of the wavelengths of several ice thicknesses is reflected as longitudinal pulls and pushes; and the difference between driving stress and the sum of basal and lateral drags is accommodated by differential longitudinal pulls and pushes, Mayer and Huybrechts (1999). But averaged over the glacier volume, positive and negative pushes and pulls from LSG largely cancel, and thus LSG does not contribute to the large-scale balance of forces, Van der Veen et al. (2014). As found by Whillans et al. (1989), the large variations in driving stress are partly resisted by the gradients in longitudinal stresses such that basal drag is spatially less variable; but there can be isolated regions of high basal drag, so called 'sticky spots'. Van der Veen and Whillans (1989b) emphasized the importance of 'sticky spots' stating that the flow of the ice-sheet is controlled by the 'sticky' sites of large drag and low slip, thus highlighting the importance of 'sticky spots'. Thus, these 'sticky spots' are influencing the large-scale dynamics of the glacier with the help of LSG. The longitudinal stress gradients modulate basal drag over much shorter distances compared to lateral drag, thereby reducing the variation of basal drag, Price et al. (2002). Thus it is seen that the spatial variability of basal drag is much less than the variations in driving stress. So the assumption of a uniform limiting basal shear stress is not likely to introduce much error in thickness calculations, and still less error in the overall volume calculation of a glacier.

In the present work, the value of τ_b (kPa) used is based on the parametrization with the elevation range ΔH as estimated empirically by Haeberli and Hoelzle (1995):

$$\tau_b = 0.5 + 159.8\Delta H - 43.5(\Delta H)^2 \;,\; \Delta H \le 1.6\ km$$
$$= 150 \quad ,\Delta H > 1.6\ km \qquad (2)$$

Linsbauer et al. (2012) and Frey et al. (2014) also used the above parametrization for basal shear stress for the calculation of ice thickness distribution for a glacier, though Li et al. (2012) tuned the value of basal shear stress using GPR thickness data. Linsbauer et al. (2012) also remarked that the large spread of the data points found in Haeberli and Hoelzle (1995) showed the general variability of flow dynamics represented by ice-creep factor and slip ratio, with the scatter of the data points showing an uncertainty of ±30% and for some individual glaciers even ±45%.

In this work, the factor f is based on the effects of lateral drag and longitudinal stress gradients on ice-velocity. The effect of lateral drag is incorporated by taking Nye shape factor $f_n = 0.8$ uniformly everywhere on the glacier. The effect of longitudinal stress gradients is taken as a product of two factors L_d and L_s. The factors L_d and L_s are explained in the next section. The overall factor f is a product of f_n, L_d and L_s. But the factor L_s depends on slip-ratio ϕ. For the zero value of slip-ratio, L_s =1 and its value decreases with increase in slip-ratio. The factor L_d depends only on the mean slope of surface at the point where calculations are made. The slope of the ice-surface at a point is calculated over a distance of about one mean ice-thickness of the glacier.

Assuming the value of vertical shear stress at bedrock as the limiting value τ_b, the vertical shear stress causing deformation in ice can be represented by $\tau_b\left(1-\frac{z}{H}\right)$ with the zero value at ice surface and the maximum value τ_b at ice-bedrock interface. The expression of surface velocity becomes, Nye (1952):

$$u_s = \frac{2A}{n+1}\tau_b^n H + u_b = (1+\phi)\frac{2A}{n+1}\tau_b^n H \qquad (3)$$

Eq. (3) has two unknowns, i.e. ϕ and H. The creep parameter A and ice surface velocity are the same as used in Eq. (1). Equations (1) and (3) are used to calculate ice-thickness H and slip ratio ϕ. In Eq. (1) and Eq. (3), there are only two independent unknowns, i.e. ϕ and H; the unknown factor f depends on the value of ϕ. Van der Veen et al. (2014) mentioned that 'sticky spots' on bedrock lead to greater ice deformational velocity, implying that deformational velocity is directly proportional to the basal drag. Deformational velocity is generated by the vertical shear stress, which can be estimated from the limiting basal shear stress. Also it is generated by the effective driving stress. Both routes should give the same result of surface velocity. That is the physical principle used in the proposed method. Nye (1952) mentioned Eq. (3) for the calculation of surface velocity based on basal shear stress. He also mentioned Eq. (1) for the calculation of surface velocity using effective driving stress. The unknowns: slip ratio ϕ and shape factor f need to be estimated.

Initially ϕ is taken as zero. With the zero value of slip ratio, the value of shape factor f is calculated with f_n =0.8, L_s =1, and L_d given by an expression depending on the bedrock slope. Now, the thickness H can be separately calculated from both the Eq. (1) and Eq. (3) as all the other unknowns are assigned some value.

The ice thickness values calculated by Eq. (1) and Eq. (3) are called H_1 and H_2 respectively. In Eq. (3), the larger value of τ_b will result in a smaller value of ice-thickness H_2 for the same surface velocity. This implies that the larger shear stress values can produce the same surface velocity in a smaller thickness of the glacier ice.

If $H_1 > H_2$, it means the basal shear stress induced by gravity is smaller than the limiting shear stress τ_b. In this situation when ice has zero sliding velocity, the maximum value of basal friction is not realized; the longitudinal stress gradients are not required to balance the driving load, and the factors L_d and L_s are made equal to 1. So the value of factor f is made equal to f_n, i.e. 0.8, just to provide for the side drag due to glacier valley walls. The thickness calculated by Eq. (1), i.e. H_1 is considered as the ice thickness in this situation.

If $H_2 > H_1$, it means that the vertical shear stress induced by self-weight is exceeding the limiting value of basal shear stress τ_b. It is assumed that this leads to slip at the ice-bed interface; also, the longitudinal stress gradients come into play and help in resisting the driving load. Now, the basal velocity or slip ratio needs to be calculated. Increase in slip ratio reduces the deformational component of ice velocity, and also decreases the factor L_s, hence reducing the fraction of driving stress causing the shear deformation of ice. The slip ratio is iteratively increased until $H_2 \sim H_1$ and the corresponding thickness is treated as ice-thickness at that point. This iterative process helps in computing the slip-ratio ϕ and shape factor f, leading to the calculation of ice-thickness. This iterative procedure helps in quantifying the non-local effects of LSG in resisting the driving stress, thus capturing the integrated effect of the physical interaction between the ice and the bedrock. The flow chart for thickness calculation is shown in Fig. 1.

Further, at the end of calculations for the volume of the glacier, the aggregate driving load is found by summing the term '$\rho g h \sin\alpha$' over each pixel area; basal drag is calculated by multiplying limiting basal shear stress τ_b with glacier area, and lateral drag is calculated as 20% of the driving load. If the ratio of aggregate driving load to the sum of basal and lateral drags is greater than 1, it means that the glacier is not in force equilibrium, and the average limiting basal stress needs to be increased. So the value of τ_b is increased and thickness calculations are performed again. This process is iterated until the glacier as a whole is seen to be in equilibrium with the basal and lateral stresses balancing the gravitational driving load of the glacier ice. The role of LSG is mainly to distribute the basal drag more evenly over the glacier bed; it would increase (decrease) the basal drag where it would otherwise have been smaller (larger), Price et al. (2002). The LSG does not contribute to large-scale balance of forces as pushes and pulls from LSG largely cancel when integrated over the entire glacier, Van der Veen et al. (2014).

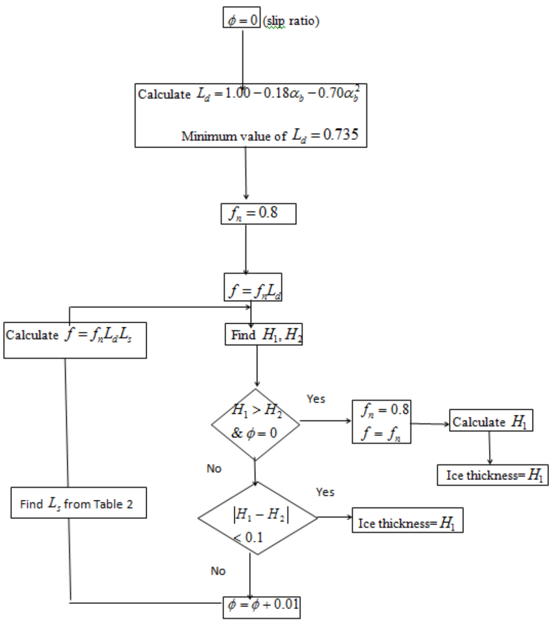

Figure 1: Flow chart for calculation of ice thickness at a point using slope and ice surface velocity data

III. *Values of L_d and L_s from the finite element simulations conducted by Adhikari and Marshall (2011)*

Slip ratio ϕ can be estimated by the iterative approach mentioned above. Adhikari and Marshall (2011) conducted a simulation study where they calculated the deformation based longitudinal stress factor L_d for the zero basal velocity, and used it to modify the shear deformational model in the same way as Nye did for incorporating the effect of lateral drag due to side walls of the glacier valley. They obtained the following equation for L_d from a quadratic fit to the data generated from the finite element simulation of plane strain Stokes model and a modified shear deformation model.

$$L_d = 1.00 - 0.18\alpha_b - 0.70\alpha_b^2 \qquad (4)$$

where α_b is the slope of the glacier bedrock. They observed that the factor L_d was relatively insensitive to the aspect ratio of the glacier; and also though the factor L_d was found by assuming a flat bed surface of uniform slope, adding roughness to the bed surface did not change L_d. In this work, the minimum value of L_d is taken as 0.735 as the expression of L_d, i.e. Eq. (4), is valid only for the intermediate range of slopes. In the present work, the slope of glacier surface is assumed to mimic the bedrock slope.

Table 5 of Adhikari and Marshall (2011) lists the values of the slip-based longitudinal stress factor L_s for different values of slip ratio ϕ and sliding length to maximum thickness ratio l_s / h ; it lists the values of L_s for different values of ϕ, but with the value of ϕ put as zero in Eq. (1). The same Table is replicated in this paper as Table 2 but with the modified values of L_s which require the non-zero value of ϕ to be substituted in Eq. (1). The factor L_s quantifies the effect of slip on the flowline velocity due to the longitudinal stress gradients; increase in ϕ reduces the value of L_s. They found that the factor L_s was not sensitive to the bedrock (or surface) slope.

In this paper, the sliding length is assumed to be proportional to the length of glacier; it is seen that assuming it as half the length provides better match between the measured thickness values and the thicknesses calculated by the proposed method. This is an important decision as it affects the thickness calculations significantly. In this work, for glacier length below 4000 m, the ratio l_s / h is taken as 2; between 4000 m and 7000 m, the ratio is taken as 5; between 7000 m and 10000 m, the ratio is taken as 10; between 10000 m and 15000 m, the ratio is taken as 20; and above the glacier length of 15000 m, the ratio is taken as 50. From Table 2, it can be clearly seen that increasing l_s / h ratio reduces the effect of LSG; the value of correction factor L_s is closer to 1 for higher l_s / h ratio for the same value of slip ratio. It is just as expected because the longer the glacier, more valid is the SIA approximation.

Though the factors L_d and L_s were computed separately by Adhikari and Marshall (2011), the former calculated by considering the ice surface as flattened half-circle with zero basal velocity, and the latter calculated by considering the glacier as a flat slab of infinite length but with a finite sliding length, they found that the two factors were compatible with each other in a problem that had the geometry corresponding to L_d but with a sliding condition at the ice/bedrock interface; the absolute difference in average velocity between the Stokes and the modified

deformational model was seen by them to be less than 4%. So it seems justified to use an overall shape factor f given by the product of f_n, L_d and L_s to find the effective driving force or net body force per unit volume in the equilibrium equation as below:

$$\sigma_{xz,z} + (f_n \, L_s L_d)\rho g \sin\alpha = 0 \qquad (5)$$

where $\sigma_{xz,z}$ is the partial derivative of stress σ_{xz} with respect to the *z*-coordinate and the equation represents force balance in the *x*-direction taken along the length of the glacier. Above equation is the governing equilibrium equation whose integration along with the Glen's flow rule results in the ice surface velocity Eq. (1).

Table 2: The longitudinal stress factor L_S based on slip ratio ϕ and ratio of sliding length to thickness l_s/h (adapted from Table 5, Adhikari and Marshall 2012)

l_s/h \ ϕ	0	0.5	1	2	3	4	5
0	1.0	0.873	0.793	0.693	0.630	0.584	0.550
2	1.0	0.886	0.818	0.732	0.674	0.632	0.599
5	1.0	0.915	0.873	0.827	0.797	0.772	0.753
10	1.0	0.945	0.923	0.901	0.863	0.875	0.865
20	1.0	0.970	0.960	0.949	0.943	0.938	0.934
50	1.0	0.988	0.983	0.979	0.977	0.975	0.974
∞	1.0	1.0	1.0	1.0	1.0	1.0	1.0

IV. *No requirement of digitizing central flowline*

The method presented in this paper can work both ways, one way is to digitize the central flowline and use calculated ice thickness to find the area of cross-section with the assumption of a parabolic or elliptic or some other shape of glacier bedrock; the other way is to find thicknesses at all image pixels of the glacier surface and find the glacier volume by adding up all the pixel volumes. The method of calculating thickness at every pixel eliminates time consumed in digitizing the central flowline and makes the process of finding volume of a glacier fully automatic.

Flowers et al. (2011) accounted for the lateral drag by parametrizing it with changes in valley width. Their flowband model assumed lateral homogeneity (rectangular cross-section) in the glacier profile. Their results were not sensitive to the choice of alternate flowlines that deviated substantially from the centerline.

Van der Veen et al. (2014) reported from their study on Byrd glacier, East Antarctica that the lateral drag varies nearly linearly across the width unless there are large variations in the bed-rock geometry across the width, thus making the effect of lateral drag almost constant in resisting the driving load. The calculation of mean local slope over the length equal to mean ice thickness is taken as the basis to justify the use of SIA based velocity equation at every pixel of the glacier surface in this work. And the influence of nonlocal effects on ice surface velocity has been taken care of by the shape factor f defined as the product of f_n, L_d and L_s. It is expected that the methodology will be less sensitive to the errors caused by the assumption of constant effect of lateral drag on surface velocity across the width. The GPR data on thickness will be helpful in assessing the errors of the method for thickness computation for points at the flowline or away from it.

V. *Calculation of surface slope and ice surface velocity*

The surface slope α is derived from the DEM and smoothed with a focal mean filter of 5×5 or 7×7 kernel size. The mean slope is calculated from the smoothed slope grid and the value is assigned to the centroid cell. The mean slope is found over a length equal to the mean ice thickness. This helps in retaining the effect of undulations with a wavelength of several ice-thicknesses, while small-scale variations are filtered. Transmission from bedrock to surface features is most efficient for the bedrock undulations of wavelengths of order of 3-5 ice thicknesses, Budd (1970) and Mayer and Huybrechts (1999).

VI. *Testing of the method on Nisqually glacier*

Nisqually glacier is a valley glacier on the south side of Mount Rainier, Washington. The glacier is 6.5 km long and the altitude range is 4360 m a.s.l. to 1410 m a.s.l. in the year 1966. Meier (1968) reported measurements of surface elevation, surface velocity and local slope at a profile 1.01 km up-glacier from the 1966 terminus at an altitude of about 1830 m where the glacier is about 610 m wide. The data was collected for the period 1943-1966. The surface elevation at the profile location varied from 1808 m to 1844 m during this period. The reported estimate of mean thickness at the profile in the year 1961 ranged from a minimum of 127 m to a maximum of 157 m.

The data reported by Meier (1968) is used in this work to test the new method.

The slope value reported is measured in the vicinity of the profile, instead of being averaged over a long distance. So in the present work, an average slope value is taken for the entire dataset. Only surface velocity is different corresponding to the year of measurement. The ice surface velocity at the profile ranges from about 16 m a^{-1} in 1948 to 134 m a^{-1} in 1963. Also slope values have been tried in the range $11^\circ - 15^\circ$ and the change in thickness studied.As the altitude range of the glacier is about 3 km, so the limiting basal shear stress value is taken as 150 kPa as per Haeberli and Hoelzle (1995) formula. Since the length of the glacier is 6.5 km, the ratio of sliding length to centerline thickness is taken as 5. The value of creep parameter A is taken as 2.4x10^{-24} $\text{Pa}^{-3}\,\text{s}^{-1}$. For the value of slope equal to 15°, the thickness of ice at the profile is calculated to be 132 m in 1961 which is within the reported range of 127-157 m. As calculated by the new method, the difference between the maximum (year 1963) and minimum (year 1948) ice thicknesses, corresponding to the respective surface velocities of 164 and 16 m a^{-1}, is about 38 m which is close to the value of 36 m reported by Meier (1968). The calculations show that the slip ratio changed from 0.3 in 1948 to 8.5 in 1963 causing a change in the correction factor due to LSG from 0.85 to 0.6, thereby increasing the ice thickness calculated for the year 1963. For the variation of $11^\circ - 15^\circ$ in the value of mean slope at the location of profile, thickness change between 1948 and 1963 lies between 38-46 m which is reasonably close to the reported difference of 36 m.

For the particular case of ice surface velocity of 164 m a^{-1} and surface slope of 15°, Table 3 lists the values of ice thickness, overall correction or shape factor f, and sliding velocity as a percent of surface velocity. Above values are listed for a combination of variables like creep parameter A, limiting basal shear stress τ_b, and sliding length to maximum thickness ratio l_s / h. Table 3 shows that the change in creep parameter A by 35% causes a 12% change in ice thickness; increase in τ_b by 33% increases ice thickness by 12%; the change in the ratio l_s / h from 5 to 10 decreases ice thickness by about 17 %. The value of % sliding velocity is seen to vary inversely with the value of τ_b. The l_s / h ratio is important in estimating the value of correction factor L_s; this ratio signifies the deviation from the SIA approximation.

So the data at a single transverse profile for each year from 1943 to 1966, reported by Meier (1968), is analysed in this work. At this profile, the glacier changed in thickness by a factor of 1/3, and in surface speed by a factor of 10. With the channel shape and bed roughness presumably constant, the range of surface speeds could only be explained by the variation of basal sliding velocity. With the assumption of a constant limiting basal shear stress, the driving load of higher thickness of ice is supported by the increased pull due to the LSG resulting from the higher slip ratio. It is assumed that increased basal velocity is causing an increase in resistance offered due to LSG rather than due to any change in basal shear stress; the factor L_s as calculated from Table 2 for different values of slip ratio helps in assessing the effect of LSG in resisting the driving load.

Table 3: Ice thickness, correction or shape factor, and percent sliding velocity for Nisqually glacier at a profile with the surface slope of 15° and velocity of 134 m a^{-1}

τ_b (k Pa)	A ($\text{Pa}^{-3}\,\text{s}^{-1}$)	l_s/h = 5	l_s/h = 10
150	1.56×10^{-24}	150 m, 0.44, 92%	118 m, 0.55, 94%
	2.4×10^{-24}	134 m, 0.49, 90 %	112 m, 0.58, 91%
	3.24×10^{-24}	126 m, 0.52, 86%	108 m, 0.60, 88%
200	1.56×10^{-24}	158 m, 0.55, 81%	140 m, 0.62, 83%
	2.4×10^{-24}	150 m, 0.58, 72%	137 m, 0.64, 74%
	3.24×10^{-24}	145 m, 0.60, 64%	135 m, 0.65, 66 %

V. RESULTS

I. Volumes of Himalayan glaciers from the new method

The method is applied to Zemu and Dokriani glaciers and the results are compared with the reported results to assess the effectiveness of the new method. Table 4 shows the comparison of volumes and mean thicknesses of Zemu and Dokriani glaciers. The volume of Zemu glacier calculated by the new method is within 30% of the values reported by different methods by Frey et al. (2014). The volume of Dokriani glacier as found from the GPR survey by Gergan et al. (1999) differs by 33% from the value from the new method. Thus it is seen that the volume results from the new method are comparable to the reported results.

Table 4: Volume (km^3) and mean thickness of a few Himalayan glaciers

$A\ (Pa^{-3}s^{-1})$ / τ_b (k Pa)	1.56×10^{-24}	2.4×10^{-24}	3.24×10^{-24}
90	127, 88% (2.17), 0.67	106, 84% (1.91), 0.60	96, 80% (1.76), 0.54
150	116, 54% (1.36),0.34	106, 42% (1.27), 0.29	99, 35% (1.21), 0.26
195	120, 28% (1.15), 0.22	109, 20% (1.06),0.18	101, 15% (<u>1.002</u>),0.15
210	121, 22% (1.089),0.19	109, 15% (<u>1.0035</u>),0.15	101, 11% (0.944),0.12
230	121, 16% (<u>0.9997</u>), 0.16	109, 10% (0.93), 0.12	101, 7% (0.87), 0.09

II. *Volume of the East Rathong glacier*

East Rathong is a glacier located in Sikkim Himalaya. Using Cartosat-1 DEM 2008 and Landsat 8 images of 2013 and 2014, the slope and ice surface velocity data of the glacier are computed. Table 5 shows the mean thickness, % basal velocity, ratio of driving load to the sum of basal and lateral drags, and ratio of aggregate pull due to LSG and driving load for East Rathong glacier for different values of τ_b and creep parameter A. The average thickness of the glacier is estimated to be 109±10 m, i.e. a variation of about 10% when there is a variation of 35% in the creep parameter value.

Table 5 shows that the influence of variability in the value of limiting basal shear stress on the volume is minimized by an accompanying change in slip ratio. The variation in volume of the glacier is only 5% for 40% variation in τ_b. But the influence of creep parameter A is significant on the volume calculated. Variation of 35% in the value of creep parameter A leads to 10% variation in the volume of glacier. The value of creep parameter can be tuned or calibrated if GPR survey data of ice thickness is available for some points on the glacier.

Table 5: Mean thickness (m), % average basal velocity and ratio of aggregate driving load to the sum of basal and lateral drags (in brackets), and ratio of resistance due to LSG and driving load for East Rathong glacier for different values of τ_b and A

	Area (km^2)	GlabTop 2 Frey et al. (2014)	HF model Frey et al. (2014)	GPR survey Gregan et al. (1999)	(Haeberli and Hoelzle 1995 method) Frey et al. (2014)	Present method
Zemu	77.3	8.4 (109 m)	9.1 (118 m)		8.1 (104 m)	6.42 19% basal velocity (83 m)
Dokriani	5.76			0.283 (50m, 1995)		0.397 14% basal velocity (67 m)

In this work, τ_b is initially calculated using the empirical relation from Haeberli and Hoelzle (1995), and volume of the glacier is computed using this value of limiting basal shear stress. At the end of calculations, the ratio of aggregate driving load to the sum of basal and lateral drags is checked. If this ratio is less than or equal to 1, the glacier is in mechanical equilibrium. Otherwise, the value of τ_b is revised and thickness calculations performed again until this ratio becomes close to 1. The average basal velocity is seen to be 15% of the surface velocity at the equilibrium situation for East Rathong glacier.

From Table 5, it is seen that the role of LSG increases with increase in slip ratio. As the limiting basal shear stress increases, slip ratio reduces and the factor L_s increases, thus resulting in reduction of resistance offered due to LSG for balancing the driving load. The contribution of LSG is mainly to redistribute the basal drag. The aggregate pull due to LSG is seen to resist about 15% of driving load for East Rathong glacier at the equilibrium situation when aggregate driving load is balanced by the sum of basal and lateral drags. This value is close to the value reported in other studies where aggregate pull from LSG is seen to redistribute about 20 % of the driving load, Price et al. (2002).

VI. DISCUSSION

The results from the new method are comparable to the reported volumes of some Himalayan glaciers. The volume calculated for the East Rathong glacier shows variation of 10% when there is a variation of 35% in the value of A. So the method is robust for volume calculation. The value of *A* can be tuned if GPR thickness data is available for some points.

The proposed method uses a modified SIA model based on incorporating the effect of lateral drag and longitudinal stress gradients on ice surface velocity. The Nye shape factor f_n is taken as 0.8 to account for the effect of lateral drag on ice-velocity. The effect of LSG is quantified by the finite element simulation results of 3-D Stokes model in the form of factors L_d and L_s as reported by Adhikari and Marshall (2011). The factor L_d is calculated from the surface slope value. The factor L_s depends on slip ratio, i.e. ratio of sliding velocity and deformational velocity. Also the factor L_s depends on a glacier parameter, i.e. its length; glacier length is important in estimating the ratio of sliding length and centerline thickness of glacier. The method uses important glacier parameters like its length and altitude range for the calculation of volume.

The method estimates the limiting mean basal shear stress τ_b from Haeberli and Hoelzle (1995) empirical relation based on the altitude range of a glacier. The value of τ_b for a glacier can be revised to enforce the global force equilibrium of the glacier under the forces of gravitational driving load, basal and lateral drags. The LSG does not contribute to the large-scale balance of forces as pushes and pulls from LSG largely cancel when summed over the glacier volume, Van der Veen et al. (2014). The assumption of a constant limiting basal shear stress was advocated in Lliboutry's theory on sliding, bed erosion and cavitation.

The calculations done for Nisqually glacier demonstrate that the increase in surface velocity by a factor of 10 could be explained by the new method by an increase in basal velocity and accompanying increase in ice thickness by a factor of 1/3. The LSG is helpful in describing the short-scale variation of surface velocity and providing improved estimates of local ice thickness. This work assumes that increase in basal velocity causes an increase in LSG, rather than any increase in basal shear stress.

The method has potential and is seen to be robust. It is hoped that the method will prove itself useful for the volume estimation of a glacier complex as well.

VII. CONCLUSIONS

The conclusions made from this study are as follows:

1. The new method of volume calculation is able to capture the high order mechanics of glaciers with the use of factors f_n, L_d and L_s.
2. The volumes of Zemu and Dokriani glaciers found by the new method are comparable with the reported values.
3. The mean ice thickness of East Rathong glacier is estimated to be 109 m.
4. The new method is quite robust for finding the volume of a glacier. The variation of 35 % in the value of creep parameter A resulted in a variation of 10 % in the volume for East Rathong glacier, while variation of 40% in the value of τ_b resulted in only a variation of 5% in the volume.
5. The new method does not require digitization of flowlines and glacier boundaries. Hence the process of volume estimation can be automated.

REFERENCES

[1] Adhikari, S. and Marshall, S.J.: Improvements to shear-deformational models of glacier dynamics through a longitudinal stress factor, *Journal of Glaciology*, 57(206), 1003–1016, 2011.

[2] Adhikari, S. and Marshall, S.J.: Parameterization of lateral drag in flowline models of glacier dynamics, *Journal of Glaciology*, 58(212), 1119–1132, doi: 10.3189/2012JoG12J018, 2012.

[3] Brinkerhoff D. J., Aschwanden A. and Tuffer M.: Bayesian Inference of subglacial topography using mass conservation, Frontiers in earth science, 4, article 8, doi: 10.3389/feart.2016.00008, 2016.

[4] Budd, W. F., Ice-flow over bedrock perturbations, *Journal of Glaciology*, 9, 55, 29-47, 1970.

[5] Cooper, A.P.R., Tate, J.W. and Cook, A.J.: Estimating ice thickness in South Georgia from SRTM elevation data, *The International Archives of the Photogrammetry, Remote Sensing and Spatial Information Sciences*, 38, Part II, 592-597, 2010.

[6] Cuffey, K. and Patterson, W.: The Physics of Glaciers, fourth edn, Butterworth Heinemann, Elsevier, 2010.

[7] Farinotti, D., Huss, M., Bauden, A., Funk, M. and Truffer, M.: A method to estimate the ice volume and ice-thickness distribution of alpine glaciers. *Journal of Glaciology*, 55(191), 422–430, 2009.

[8] Flowers, G.E., Roux N., Pimentel, S. and Schoof, C.G.: Present dynamics and future prognosis of a slowly varying glacier, *The Cryosphere*, 5, 299-311, 2011.

[9] Fowler, A.C.: Weertman, Lliboutry and the development of sliding theory, *Journal of Glaciology*, 56 (200), 965-972, 2010.

[10] Frey, H., Machguth, H., Huss, M., Huggel, C., Bajracharya, S., Bolch, T., Kulkarni, A., Linsbauer, A., Salzmann, N. and Stoffel, M.: Estimating the volume of glaciers in the Himalayan–Karakoram region using different methods, *The Cryosphere*, 8(6), 2313–2333, 2014.

[11] Gantayat, P., Kulkarni, A.V. and Srinivasan, J.: Estimation of ice thickness using surface velocities and slope: case study at Gangotri Glacier, India, *Journal of Glaciology*, 60(220), 277–282, 2014.

[12] Gergan, J.T., Dobhal, D.P. and Kaushik, R.: Ground penetrating Radar ice thickness measurements of Dokriani-bamak glacier, Garhwal Himalayas, *Current Science*, 77(1), 169-174, 1999.

[13] Haeberli, W. and Hoelzle, M.: Applications of inventory data for estimating characteristics of regional climate-change effects on mountain glaciers: A pilot study with the European Alps, *Annals of Glaciology*, 21, 206-212, 1995.

[14] Kamb, B. and Echelmeyer, K.A.: Stress-gradient coupling in glacier flow: I. Longitudinal averaging of the influence of ice thickness and surface slope, *Journal of Glaciology*, 32(111), 267-284, 1986.

[15] Li, H., Ng, F., Li, Z., Qin, D. and Cheng, G.: An extended “perfect-plasticity” method for estimating ice thickness along the flow line of mountain glaciers, *Journal of Geophysical Research*, 117, F01020, doi: 10.1029/2011JF002104, 2012.

[16] Linsbauer, A., Paul, F. and Haeberli, W.: Modeling glacier thickness distribution and bed topography over entire mountain ranges with GlabTop: Application of a fast and robust approach, *Journal of Geophysical Research*, 117(F3), p.F03007, doi: 10.1029/2011JF002313, 2012.

[17] Mayer, C. and Huybrechts, P.: Ice-dynamic conditions across the grounding zone, Ekstromisen, East Antarctica,. *Journal of Glaciology*, 45(150), 384-393, 1999.

[18] McNabb R. W., Hock R., O'neel S., Rasmussen L. A., Ahn Y., Braun M., Conway H., Herreid S., Joughin I., Pfeffer W. T., Smith B. E., and Truffer M.: Using surface velocities to calculate ice thickness and bed topography: a case study at Columbia Glacier, Alaska, USA, J. of Glaciology, 58, 1151-1164, doi: 10.3189/2012JoG11J249, 2012.

[19] Meier, M.F.: Calculations of slip of Nisqually glacier on its bed: no simple relation of sliding velocity to shear stress, *Int. Assoc. Sci. Hydrol*., Bern General Assembly, 1967, Pub 79, 49-57, 1968.

[20] Meur, E.L., Gagliardini, O., Zwinger, T. and Ruokolainen, J.: Glacier flow modelling: a comparison of the SIA and the full-Stokes solution, *C. R. Physique*, 5, 709-722, 2004.

[21] Meur, E.L. and Vincent, C.: A 2-D shallow ice-flow model of Glacier de Saint-Sorlin, France. *Journal of Glaciology*, 49(167), 527-538, 2003.

[22] Morlighem M., Rignot E., Seroussi H., Larour E., Ben Dhia H., and Aubry D.: A mass conservation approach for mapping glacier ice thickness, Geophysical Research Letters, 38, L19503, doi: 10.1029/2011GL048659, 2011.

[23] Nye, J.F.: The mechanics of glacier flow. *Journal of Glaciology*, 2, 82-93, 1952.

[24] Nye, J.F.: The flow of a glacier in a channel of rectangular, elliptic or parabolic cross-section, *Journal of Glaciology*, 5(4), 661-690, 1965.

[25] Price, S.F., Bindschadler, R.A., Hulbe, C.L. and Blankenship, D.D.: Force balance along an inland tributary and onset to Ice Stream D, West Antarctica, *Journal of Glaciology*, 48, 20-30, 2002.

[26] Truffer, M.: The basal speed of valley glaciers: an inverse approach, *Journal of Glaciology*, 50(169), 236-242, 2004.

[27] Van der Veen, C.J., Stearns, L.A., Johnson, J. and Csatho, B.: Flow dynamics of Byrd glacier, East Antarctica, *Journal of Glaciology*, 60(224),1053-1064, 2014.

[28] Van der Veen, C.J. and Whillans, I.M.: Force Budget: I. Theory and Numerical methods, *Journal of Glaciology*, 35(119), 53-60, 1989a.

[29] Van der Veen, C.J. and Whillans, I.M.: Force Budget: II. Application to 2-d flow along Byrd station strain network, Antarctica, *Journal of Glaciology*, 35(119), 61-67, 1989b.

[30] Vincent, C., Vallon, M., Reynaud, L. and Meur, E.L.: Dynamic behavior analysis of glacier de Saint-Sorlin, France, from 40 years of observations, 1957-97, *Journal of Glaciology*, 46(154), 499-506, 2000.

[31] Whillans, I.M., Chen, Y.H., Van der Veen, C.J. and Hughes, T.J.: Force budget: III. Application to three-dimensional flow of Byrd glacier, Antarctica, *Journal of Glaciology*, 35(119), 68-80, 1989.